



Is burn severity related to fire intensity? Observations from landscape scale remote sensing

Journal:	<i>International Journal of Wildland Fire</i>
Manuscript ID:	WF12087.R4
Manuscript Type:	Research Paper
Date Submitted by the Author:	n/a
Complete List of Authors:	Heward, Heather; University of Idaho, Department of Forest, Rangeland, and Fire Sciences Smith, Alistair; University of Idaho, Dept of Forest Resources Roy, David; South Dakota State University, Geographic Information Science Center of Excellence Tinkham, Wade; University of Idaho, Department of Forest, Rangeland, and Fire Sciences Hoffman, Chad; Colorado State University, Forest and rangeland stewardship Morgan, Penny; University of Idaho, Department of Forest, Rangeland, and Fire Sciences; University of Idaho, Dept, of Forest Resources Lannom, Karen; University of Idaho, Department of Forest, Rangeland, and Fire Sciences
Keyword:	Remote sensing, Fire intensity, Burn severity

SCHOLARONE™
Manuscripts



1 Title: **Is burn severity related to fire intensity? Observations from landscape scale remote**
2 **sensing**

3

4 Suggested Running Head: **Is burn severity related to fire intensity**

5

6 Heather Heward^{1‡}, Alistair M.S. Smith^{1*‡}, David P. Roy^{2‡}, Wade T. Tinkham¹, Chad M.

7 Hoffman³, Penelope Morgan¹, and Karen O. Lannom¹.

8

9 ¹Department of Forest, Rangeland, and Fire Sciences, University of Idaho, Moscow, ID, USA;

10 emails: hheward@gmail.com; alistair@uidaho.edu, tink8633@vandals.uidaho.edu,

11 pmorgan@uidaho.edu, klannom@uidaho.edu

12 ²Geographic Information Science Center of Excellence, South Dakota State University,

13 Brookings, SD, USA; email: david.roy@sdstate.edu

14 ³Department of Forest and Rangeland Stewardship, Colorado State University, Fort Collins, CO,

15 USA; email: c.hoffman@colostate.edu

16

17

18 **Abstract**

19 Biomass burning by wildland fires has significant ecological, social, and economic impacts. Satellite
20 remote sensing provides direct measurements of radiative energy released by the fire (i.e. fire
21 intensity) and surrogate measures of ecological change due to the fire (i.e. fire/burn severity).
22 Despite anecdotal observations causally linking fire intensity with severity, the nature of any
23 relationship has not been examined over extended spatial scales. We compare fire intensities
24 defined by MODIS Fire Radiative Power (MODIS FRP) products with Landsat-derived spectral
25 burn severity indices for sixteen fires across a vegetation structure continuum in the western
26 United States. Per-pixel comparison of MODIS FRP data within individual fires with burn
27 severity indices is not reliable due to known satellite temporal and spatial FRP undersampling.
28 Across the fires, 69% of the variation in RdNBR was explained by the 90th percentile of MODIS
29 FRP. Therefore, distributional MODIS FRP measures (median and 90th-percentile FRP) derived
30 from multiple MODIS overpasses of the actively burning fire event may be used to predict
31 potential long term negative ecological effects for individual fires.

32

33 **Table of contents summary**

34 This study compares fire intensities defined by MODIS Fire Radiative Power (MODIS FRP)
35 products with Landsat-derived spectral burn severity indices for sixteen fires. When analyzing
36 data with individual fires as the experimental unit, relationships between fire intensity and burn
37 severity are presented.

38

39 * Corresponding Author; Email: alistair@uidaho.edu

40 ‡ Denotes equal contribution

41

42 Introduction

43

44 Biomass burning from wildland fires is a critical component of the Earth system and
45 results in significant atmospheric, social, ecological, and economic impacts; some immediate and
46 several that last decades. Fires are also amongst the largest point source emitters of trace gas and
47 aerosols to the atmosphere and are inherently variable in their timing, geographic extent, and
48 effects (Giglio *et al.* 2010; Roy *et al.* 2008; van der Werf *et al.* 2010). Fire continues to be a
49 topic of public and policy concern in the United States; especially through the expansion of the
50 wildland urban interface where human-natural systems converge (Daniel *et al.* 2007; Paveglio *et*
51 *al.* 2009). Despite intensive efforts at fire suppression, the western United States has
52 experienced extensive fires in recent decades, with the area burned and occurrence of extreme
53 fires expected to increase due to predicted changes in climate (Westerling *et al.* 2006; Littell *et*
54 *al.* 2009). An improved understanding of these fires' characteristics and how social-ecological-
55 systems recover through time are required to provide land managers and policy makers the
56 information needed to prepare for, or mitigate, the impacts of these events.

57 The burn severity of wildland fires can have significant effects on long-term (decadal)
58 vegetation structure (Goetz *et al.* 2007), eco-hydrological processes (Adams *et al.* 2012), and
59 social systems (McCool *et al.* 2006). Definitions of severity vary, but is usually defined loosely
60 as “*the magnitude of ecological change due to the fire*” (Lentile *et al.* 2006), or more
61 quantitatively via metrics such as mortality of dominant vegetation, depth of litter/duff
62 consumption, changes in species composition, etc (Conard *et al.*, 2002; Miller and Yool, 2002).
63 The term *fire severity* is often used to infer vegetation and soil changes that occur within the
64 time frame of minutes to hours (Smith *et al.* 2005). In contrast, *burn severity* is often reserved

65 for describing the impact of the fire over extended time frames of weeks to decades (Lentile *et*
66 *al.* 2006; Keeley *et al.* 2008). Spatially explicit maps of burn severity, especially immediately
67 following wildland fire events, are needed to assist land management planners in determining
68 where to effectively allocate rehabilitation resources (Robichaud 2004). However, a complete
69 understanding of the fire's severity may not be directly measurable until an extended period of
70 time after fire occurrence. Fire severity is often estimated by visual or measured field
71 observation of a number of ecological parameters (Key and Benson 2006) and burn severity is
72 often inferred using multi-temporal (pre and post-fire) airborne or satellite remotely sensed
73 spectral indices (Roy *et al.* 2006, Lentile *et al.* 2006, French *et al.* 2008).

74 The term *fire intensity* refers to the rate of heat released during the fire and can be
75 measured *in-situ* using thermocouples and thermal cameras (Smith *et al.* 2005) or at extended
76 spatial scales using airborne and satellite remotely sensed observations of the actively burning
77 fire (Smith and Wooster 2005). Fire intensity and fire/burn severity have anecdotally been
78 considered to be related, with more intense fires generally expected to cause more severe post-
79 fire effects. To date, however, this has not been examined quantitatively at landscape scales over
80 a large number of fires with varying fire behavior. If satellite retrieved fire intensity and burn
81 severity estimates are related then the relationship could provide new ways to predict potential
82 areas of long-term negative ecological effects such as increases in tree mortality, worsening soil
83 erosion, or other extended post-fire effects (Lentile *et al.* 2006).

84 In this paper we aim to quantify and understand the relationship between satellite derived
85 surrogates of burn severity and fire intensity using data at both MODIS FRP pixel and per-
86 fireextents. Satellite derived fire intensity measures (MODIS fire radiative power data) are
87 compared with burn severity estimates (as defined via Landsat spectral indices) for sixteen fires

88 across four broad vegetation types (herbaceous grassland, herbaceous shrub steppe, open tree
89 canopy, closed tree canopy).

90

91 **Background**

92

93 *Fire Intensity*

94

95 Conventionally the energy released during a fire has been characterized by fire line
96 intensity (*FLI*: kWm^{-1}) measures that area function of the heat released within the fuel that
97 burned and the rate of spread of the fire front (Byram 1959). *Byram's* fire intensity model can be
98 considered as the energy output from a strip of the actively combusting area, 1 m in length, that
99 extends from the leading edge of the fire front to the rear of the flaming zone. Another similar
100 measure of the energy released during a fire is the heat release rate per unit area (kWm^{-2}), also
101 called the *fire* reaction intensity (Rothermel 1972). The use of fire reaction intensity is common
102 in several United States fire prediction systems (Ryan 2002; Sullivan 2009a, b, c). A third
103 measure is the Fire Radiative Power (*W*) that describes the energy radiated by the fire per unit
104 time, and may be retrieved at the locations of remotely sensed active fire detections from mid-
105 infrared wavelength remotely sensed data (Kaufman *et al.* 1996). Laboratory studies of the fire
106 radiative power (FRP) integrated over time have shown a strong linear relationship with the rate
107 of fuel consumption (Wooster 2002; Freeborn *et al.* 2008; Kremens *et al.* 2010, 2012)
108 supporting suppositions that FRP could be considered as a remote measure of the fire intensity
109 (Smith and Wooster 2005; Wooster and Zhang 2004).

110

111 *Burn Severity*

112

113 Burn severity is often assessed at landscape scales via remote sensing mapping methods
114 and is commonly applied by land management agencies to describe post-fire effects under the
115 broad terms of high, moderate, and low burn severity (French *et al.* 2008). These broad
116 qualitative descriptors are used to drive the identification of priority areas for post-fire
117 rehabilitation efforts to limit soil erosion, restore plant communities, and prevent the
118 establishment of invasive or noxious species (Robichaud 2009). Parameters used to estimate
119 burn severity *in situ* include the condition and color of the soil, the amount of fuel (duff, litter,
120 surface and canopy fuels) consumed, resprouting from burned plants, consumption, mortality,
121 blackening or scorching of trees and shrubs, depth of burn in the soil, and changes in fuel
122 moisture (Key and Benson 2006; De Santis and Chuvieco 2009; Keeley *et al.* 2008). Although
123 several of these parameters are not amenable to optical wavelength remote sensing or may not be
124 related in a linear way to reflectance (Royet *et al.* 2006; Disney *et al.* 2011); field-based estimates
125 of burn severity (e.g., Composite Burn Index) are widely used to determine class breaks within
126 the remote sensing products. The majority of these methods employ multi-temporal spectral
127 indices (*unitless*) and most commonly the temporal differences in the normalized burn ratio
128 (NBR) and variants thereof (Table 1; Lentile *et al.* 2006; French *et al.* 2008).

129 The normalized burn ratio (NBR) was developed originally to detect burned areas, rather
130 than to evaluate the variations within them (López Garcia and Caselles 1991) and past research
131 has highlighted significant challenges with using this index for burn severity assessments (Roy *et*
132 *al.* 2006; Smith *et al.* 2007; French *et al.* 2008; Lentile *et al.* 2009; Smith *et al.* 2010). However,
133 other studies have shown reasonable empirical relationships ($\sim r^2 = 0.7$) between field-based tree

134 mortality and multi-temporal changes in these indices (Lentile *et al.* 2009; Keeley 2009);
135 especially in western United States ecosystems. As such, these relationships should only be
136 considered appropriate for coarsely-defined (high, moderate, and low) burn severity
137 classifications and are only applicable reliably where and when the relationships are calibrated
138 with field data (French *et al.* 2008).

139

140 *Linking Fire Intensity and Burn Severity*

141

142 It is often remarked that fire intensity is correlated with fire or burn severity (Drewa
143 2003; Smith *et al.* 2005; Keeley 2009). This supposition is logical, as more intense fires are
144 generally expected to have more significant post-fire effects and anecdotal observations support
145 this. For example, high fire intensity crown fires tend to produce areas of high tree mortality,
146 albeit in patches (Morgan *et al.* 2001). Higher intensity fires led to reduced resprouting of
147 *Adenostoma fasciculatum* (Rosaceae) in chaparral systems (Borchert and Odion, 1995) and
148 similar responses are observed for African savannabrush species (Trollope and Tainton, 1986).
149 In contrast, grass species regrow even after very high intensity fires (Trollope and Tainton,
150 1986), leading to studies characterizing severity in terms of nitrogen fluxes within such systems
151 (Smith *et al.* 2005). However, previous small area studies comparing metrics of fire intensity to
152 fire effects observed few quantitative links (Ryan and Noste 1985; Hartford and Frandsen 1992;
153 Smith *et al.* 2005) and others have observed that although the fire line intensity was "an
154 indicator" of some aboveground fire effects, it was not sufficient to fully characterize the
155 resultant impacts on soil and vegetation (Alexander 1982; Hartford and Frandsen 1992). These
156 prior observations covered a range of ecosystems including woodland and open African

157 savannahs (Smith *et al.* 2005) to conifer dominated forests of the western United States (Ryan
158 and Noste, 1975; Hardford and Fransden, 1992).

159 Arguably, fire intensity and burn severity are two examples of a fire's magnitude and are
160 not necessarily related beyond observations that high values of each metric tend to occur
161 concurrently (Ryan 2002). Moreover, satellite retrievals of fire intensity and burn severity are
162 imperfect. The fire intensity retrieved from satellite data is sensitive to satellite temporal and
163 spatial undersampling due to infrequent satellite overpasses, cloud and smoke obscuration, and
164 failure to detect cool and/or small fires (Boschetti and Roy 2009; Kumar *et al.* 2011) and satellite
165 retrieved burn severity is dependent on the change in reflectance, the proportion of the satellite
166 pixel that burned, the degree of combustion completeness, and the reflectance of the pre-fire and
167 unburned pixel components (Roy and Landmann 2005; Smith *et al.* 2005; Roy *et al.* 2010; Smith
168 *et al.* 2010).

169

170 **Methods**

171

172 Sixteen fires that occurred in the summer months of 2005 and 2006 in the western United
173 States were selected based on the availability of fire progression maps and ground truth
174 observations. The fires ranged from 400 to 50,000 ha in size (Fig. 1) and based on preliminary
175 assessment of the fire data encompassed a wide range of burn severities and fire intensities.
176 Daily fire perimeters were acquired from the United States National Interagency Fire Center
177 (NIFC) (<http://www.nifc.gov/>). The pre-fire vegetation cover for each fire was characterized
178 using the 30-m LANDFIRE data (<http://www.landfire.gov/>) ten class nomenclature defined by
179 the United States Geological Survey National Vegetation Classification System (NVCS)

180 (<http://biology.usgs.gov/npsveg/nvcs.html>). By overlaying the LANDFIRE data layers, pixels
181 within each fire were then assigned the classes: open tree canopy (25-60% canopy cover), closed
182 tree canopy (60-100% canopy cover), herbaceous grassland, or shrub steppe. Closed tree cover
183 classes included only conifers, while open included both conifers and hardwoods. Herbaceous
184 grassland included grassland, exotic herbaceous, and agricultural NVCS land cover classes.

185

186 <Insert Fig. 1 near here>

187

188 Spectral indices used to define burn severity by the USGS data were collated from the
189 Monitoring Trends in Burn Severity (MTBS) project for each of the 16 fires (MTBS:
190 <http://www.mtbs.gov/index.html>). As part of the MTBS protocol (Eidenshink *et al.* 2007), the
191 Differenced Normalized Burn Ratio (dNBR) (Key and Benson 2006) and the relative version
192 (RdNBR), developed for non-forested ecosystems (Miller and Thode 2007) are computed using
193 30-m spatial resolution Landsat imagery (Table 1). All Landsat 30-m pixels affected by clouds,
194 cloud shadows, and data gaps are discarded (Eidenshink *et al.* 2007).

195

196 <Insert Table 1 near here>

197

198 The MTBS spectral indices are computed from Landsat data acquired as soon as possible
199 (up to 16 days) after the fire occurrence and approximately one year before in the same season
200 and under approximately similar phenological conditions (Eidenshink *et al.* 2007). The MTBS
201 dNBR products are calculated with top-of-atmosphere (i.e., at sensor) reflectance that have not
202 been corrected for atmospheric effects which is a limitation of contemporary burn severity dNBR

203 mapping assessments using multi-temporal imagery if the atmosphere is variable. However,
204 atmospheric scattering in the Landsat 0.76 - 0.90 μm and 2.08 - 2.35 μm wavelengths used to
205 generate the NBR suite of indices is generally low making atmospheric impacts less of a concern
206 (Cocke *et al.* 2005; Ju *et al.* 2012).

207 The most recently available MODIS collection 5 global monthly 1km fire location
208 product (MCD14ML) (Giglio 2010) that is derived from the MODIS active fire product (Giglio
209 *et al.* 2003) was used. The product summarizes the MODIS Terra (10:30 am and pm Equatorial
210 overpass time) and MODIS Aqua (13:30 am and pm Equatorial overpass time) active fire
211 detections, providing, at the study area latitude, up to four detections and corresponding FRP
212 estimates per day. In order to ensure correct spatial correspondence between the 30m Landsat
213 burn severity measures and the MODIS FRP data the relative geometry of the two sensor data
214 were taken into account. The MODIS is a whiskbroom sensor with a 110° field of view (i.e., scan
215 angles $\pm 55^\circ$) and so the MODIS active fire product detects fires that occur in pixels that increase
216 in area from approximately 1 by 1 km at nadir to up to 2.0 by 4.8 km in the along-track and
217 along-scan directions at scan edge respectively (Wolfe *et al.* 1998). The MODIS geolocation
218 accuracy is 50m (1σ) at nadir (Wolfe *et al.* 2002). Landsat sensors have a 15° field of view (i.e.
219 scan angles $\pm 7.5^\circ$) and the change in pixel size as a function of scan angle is negligible and the
220 Landsat geolocation accuracy is less than one 30m pixel within the United States (Lee *et al.*
221 2004). A fire can occur anywhere within a MODIS pixel and its detection is dependent on a
222 number of factors including the fire temperature and size, and the flaming fire front position
223 relative to the along track MODIS triangular point spread function (Kaufman *et al.* 1998, Giglio
224 2010). Ichoku and Kaufman (2005) provide formulae for the MODIS pixel size as a function of
225 scan angle and using them the MODIS pixel area is 50% greater than at nadir for scan angles

226 greater than 27° . Consequently in this study (i) only the MODIS FRP data for MODIS active fire
227 detections with scan angles $\leq 27^\circ$ were used, (ii) a circular buffer with a radius of 0.5 km was
228 placed around each of the remaining MODIS active fire detection pixel center locations, (iii)
229 only the MODIS active fire detections falling within each fire perimeter were considered. In this
230 way we have confidence that only the 30m dNBR and RdNBR burn severity
231 values corresponding to the MODIS FRP data for the same fire events are compared.

232 Any part of the 0.5 km circular buffer that extended beyond the fire perimeter was
233 clipped and not considered in the analysis. The MODIS FRP (units: MW) is derived using a
234 nonlinear empirical relationship between the FRP and brightness temperature retrieved in the
235 mid-infrared (Kaufman *et al.* 1998). The MODIS FRP is known to be sensitive to several factors
236 including the presence of atmospheric water vapor, the fire background characterization used in
237 the FRP retrieval algorithm and the sub-pixel location of the fire and the sensing system point
238 spread function (Wooster *et al.* 2005; Schroeder *et al.* 2010). All these factors introduce
239 uncertainty into the subsequent analysis.

240 The mean dNBR and the mean RdNBR were calculated from all the 30-m Landsat pixels
241 falling within the buffer region of each 1-km MODIS active fire detection. These mean burn
242 severity values, which are co-located with active fire detections, were compared with the 1-km
243 MODIS FRP (fire intensity values). A total of 1716 individual 1-km MODIS FRP values sensed
244 across all sixteen fires during the summer months of 2005 and 2006 were available with scan
245 angle $\leq 27^\circ$. The two MODIS sensors usually have insufficient overpass frequency to provide
246 MODIS FRP estimates that characterize the evolution of the fire behavior at a fixed 1km location
247 and so the MODIS FRP values from multiple overpasses of the entire burned area or over many
248 burned areas are derived (Roberts *et al.* 2009; Kumar *et al.* 2011).

249 In this paper distributional statistics (median, maximum, and 90th-percentile) of the
250 MODIS FRP values were derived for each of the 16 fires. The maximum MODIS FRP is of
251 interest to researchers as the maximum fire intensity affects vegetation processes like grass and
252 tree response to fire (Trollope and Tainton 1986, Archibald *et al.* 2010). The 90th-percentile
253 MODIS FRP value was extracted to also capture this information as the maximum MODIS FRP
254 value might only be associated with a singularly extreme fire behavior event (such as blowups,
255 rotating vertical plumes, etc) that may only occupy a small spatial extent within the fire.
256 Spatially, the fire might exhibit numerous patches of high fire intensity, which would not be
257 captured by a maximum. Similarly, the median (the 50th-percentile) is of interest as a measure of
258 the overall fire intensity within the fire.

259 The median, maximum, and 90th-percentile MODIS FRP were compared to the mean of
260 the 1-km RdNBR and to the mean of the 1km dNBR burn severity estimates for all the pixels
261 within each individual fire (Table 2). Fires with less than 10 samples were not included. These
262 data were also analyzed by four vegetation classes: herbaceous grassland, herbaceous shrub
263 steppe, open tree canopy (25-60%), and closed tree canopy (60-100%). Insufficient individual
264 fires were available in herbaceous cover classes (n=3) to enable a reliable investigation. Linear
265 and nonlinear regression models (logarithmic, power, cubic, quadratic, etc.) within the SPSS
266 statistical package (Curve Estimation tool, Version 20, IBM Corp., New York) were used to find
267 the model of best fit. All relationships were assessed at the 95th-confidence level. The coefficient
268 of determination (r^2) and standard error of the estimate were used to evaluate different model
269 fits.

270

271

272

273 **Results and Discussion**

274

275 Fig. 2 shows scatter plots of mean 1-km RdNBR and dNBR against fire radiative power
276 for all the 1-km MODIS pixels within all 16 fires. Both the RdNBR and dNBR are poorly related
277 to the MODIS FRP at this scale. This is in part due to temporal sampling differences. Burn
278 severity methods, collected either by satellite imagery methods such, RdNBR and dNBR, or *in-*
279 *situ* (e.g., composite burn index), are principally measured following the fire. They integrate the
280 effects that occurred before the fire, during the fire combustion phases, and any post-fire
281 processes into a single time-integrated measure. In contrast, fire intensity retrieved from
282 MODIS FRP provides a temporally discrete measure at the time of satellite overpass, typically
283 during the active combustion phase as detections require sufficient radiant energy to be released.
284 These temporal samples are unlikely to capture the instances of maximum fire intensity as
285 observed throughout the lifetime of the fire and typically high MODIS FRP values occur less
286 frequently than low MODIS FRP values (Kumar *et al.* 2011). In addition, these differences may
287 be due to the different spatial resolution of the MODIS active fire detections (nominally 1km at
288 nadir) and the 30-m spatial resolution of Landsat, as aggregation of the 30-m pixels to the 1-km
289 scale will reduce variability.

290 The data illustrated in Fig. 2 indicates that the variation in the mean burn severity metrics
291 decreases with greater MODIS FRP. This pattern was found for the four vegetation cover
292 classes and for individual fires (Fig. 3). Similar patterns with *in situ* field metrics of burn
293 severity and fire intensity have been observed in past studies (Smith *et al.* 2005). These results
294 are somewhat expected as low intensity fires generally result in a wide range of spatially

295 heterogeneous ecological effects (pockets of white ash, mortality, light char, unburned, etc);
296 whereas high intensity fires often lead to more spatially homogenous impacts across contiguous
297 areas of the fire (vegetation mortality, exposure of mineral soil, etc) (Lentile *et al.* 2006). We
298 recognize that this could also be associated with errors in the MODIS FRP which can be
299 underestimated depending on the sub-pixel location of the active fire with respect to the
300 central pixel location (Schroeder *et al.* 2010), the presence of atmospheric water vapor (Wooster
301 *et al.* 2005), and because at high MODIS scan angles only larger and/or hotter actively burning
302 fires tend to be detected (Giglio *et al.* 1999; Freeborn *et al.* 2011) and they tend to have lower
303 FRP (Kumar *et al.* 2011).

304

305 <Insert Fig. 2 near here>

306 <Insert Fig. 3 near here>

307

308 Table 2 summarizes relationships between both dNBR and RdNBR with the 90th-
309 percentile and median MODIS FRP for all fires and within tree canopy cover classes. The
310 underlying assumption of these comparisons is that the distributional statistics for each of the
311 fires captures the prevailing fire behavior and ecological effects. No significant relationships
312 were found between the burn severity metrics and maximum MODIS FRP and so these results
313 are not tabulated. This indicates that singularly observed high values of MODIS FRP, such as
314 may arise from extreme fire behavior are not indicative of the overall fire behavior and effects;
315 although this could also be because at the time of satellite overpass the fire was not burning with
316 maximum fire intensity and the peaks were undersampled (Kumar *et al.* 2011). Overall, MODIS
317 FRP was a better predictor of RdNBR than dNBR (Table 2). RdNBR was designed to capture

318 the relative change in biomass while MODIS FRP provides a measure of the quantity of fuel
319 combusted (Kaufman *et al.* 1996). In contrast, dNBR provides an estimate of the relative change
320 in vegetation and soil/char cover (Lentile *et al.* 2009; Smith *et al.* 2010).

321

322 <Insert Table 2 near here>

323

324 Fig. 4 shows that within the two tree cover classes the median and 90th-percentile MODIS
325 FRP per fire are reasonable predictors of RdNBR where as across all cover classes the 90th-
326 percentile MODIS FRP is a reasonable predictor. In each case an asymptote is observed in the
327 RdNBR values indicating a lack of index sensitivity at higher fire intensities. This asymptote has
328 also been observed in numerous field studies (Cocke *et al.* 2005; French *et al.* 2008). Across the
329 fires, 69% of the variation in RdNBR was explained by the 90th-percentile of MODIS FRP
330 (Table 2 and Fig. 4). Thus, misrepresentation of predicted burn severity due to satellite MODIS
331 FRP sampling issues may potentially be overcome by use of MODIS FRP distributional
332 statistics.

333

334 <Insert Fig. 4 near here>

335

336 These results highlight further challenges beyond those already described with the usage
337 of dNBR and RdNBR to assess post-fire effects at landscape scales. The rapid asymptote of
338 RdNBR at FRP values lower than 1/3rd of the data range highlights the general insensitivity of
339 this burn severity index to fire intensity. This observed insensitivity and the broad limitations in
340 the dNBR family of spectral indices that have been discussed suggest that they should only be

341 linked to specific post-fire effects at each fire location (e.g., tree mortality) and then subsequent
342 discussions should only describe trends in that effect (e.g., Miller et al 2008).

343

344 **Conclusions**

345 Distributional measures of MODIS FRP have potential to predict potential high severity
346 and long term negative ecological effects (as indicated by RdNBR in this case) when applied at
347 the extended spatial-temporal scales of individual wildland fire events. Overall, MODIS FRP
348 was a better predictor of RdNBR than dNBR, potentially indicating a closer mechanistic link. To
349 avoid MODIS FRP temporal and spatial under-sampling (Boschetti and Roy 2009; Kumar *et al.*
350 2011) this work illustrates that MODIS FRP data should not be evaluated on a 1-km pixel scale
351 to relate to Landsat-derived RdNBR or dNBR. In other regions, especially at high boreal
352 latitudes where MODIS overpasses many times per day and where fires can burn for many days
353 this may not be the case. MODIS is used in regional, national, and global assessments of fire
354 occurrence and extent. As a result, the MODIS FRP distributional statistics could provide
355 continental scale predictions of burn severity per fire. Such information could potentially be used
356 within national fire management budget planning programs, such as Fire Program Analysis
357 (FPA) used within the United States, to help predict post-fire recovery and rehabilitation costs. In
358 order to understand the fine scale variability of fire intensity it may be worth investigating the
359 spatial distribution of burn severity metrics within individual MODIS FRP pixels. To overcome
360 the spatial and temporal integration challenges of comparing burn severity to fire intensity, field
361 research is also warranted to coincidentally measure *in situ* active fire behavior with prior fuels
362 and post-fire ecological effects. Further research is needed to develop new severity indices that
363 exhibit greater sensitivity as a function of fire behavior and ecological (and spectral) change.

364

365 **Acknowledgements**

366

367 This work was partially supported by the NSF Idaho EPSCoR Program and by the National
368 Science Foundation under award number EPS-0814387. Partial funding support was received via
369 Joint Fire Sciences Program under award number 07-2-1-60 and the National Aeronautics and
370 Space Administration (NASA) under award NNX11AO24G. This work is also recognizes the
371 support of NASA and USGS for the satellite imagery. A special thanks also to Louis Giglio for
372 his assistance with the usage of the MODIS data products.

373

374

375 **References**

- 376 Adams HD, Luce CD, Breshears DD, Allen CD, Weiler M, Hale VC, Smith AMS, Huxman TE
377 (2012) Ecohydrological consequences of drought- and infestation-triggered tree die-off:
378 insights and hypotheses, *Ecohydrology* **5**, 2, 145-159. doi: 10.1002/eco.233.
- 379 Alexander ME (1982) Calculating and interpreting forest fire intensities, *Canadian Journal of*
380 *Botany* **60**, 4, 349-357.
- 381 Archibald S, Scholes RJ, Roy DP, Roberts G, Boschetti L (2010) Southern African fire regimes
382 as revealed by remote sensing, *International Journal of Wildland Fire* **19**, 7, 861–878, doi:
383 10.1071/WF10008.
- 384 Borchert MI, Odion, DC (1995) Fire intensity and vegetation recovery in chaparral: a review, 91-
385 100, in *Bushfire in California Wildlands: Ecology and Resource Management*, Edited by JE
386 Keeley and T Scott, 1995, International Association of Wildland Fire, Fairfield, WA.
- 387 Boschetti L, Roy DP (2009) Strategies for the fusion of satellite fire radiative power with burned
388 area data for fire radiative energy derivation, *Journal of Geophysical Research* **114**,
389 D20302, doi:10.1029/2008JD011645.
- 390 Byram GM (1959) Combustion of forest fuels. In Davis, K.P. (Ed.), *Fire: Control and Use*. New
391 York: McGraw Hill.
- 392 Cocke AE, Fule PZ, Crouse JE (2005) Comparison of burn severity assessments using
393 Differenced Normalized Burn Ration and ground data, *International Journal of Wildland*
394 *Fire* **14**, 2, 189-198, doi: 10.1071/WF04010.
- 395 Conard SG, Sukhinin AI, Stocks BJ, Cahoon DR, Davidenko EP, Ivanova GA (2002)
396 Determining effects of area burned and fire severity on carbon cycling and emissions in
397 Siberia. *Climate Change* **55**, 197-211.

- 398 Daniel TC, Carroll MS, Moseley C, Raish C, eds. (2007) *People, Fire and Forests: A Synthesis*
399 *of Wildfire Social Science*, Corvallis, OR: Oregon State University Press.
- 400 De Santis A, Chuvieco E (2009) GeoCBI: A modified version of the Composite Burn Index for
401 the initial assessment of the short-term burn severity from remotely sensed data, *Remote*
402 *Sensing of Environment* **113**, 3, 554-562, doi: 10.1016/j.rse.2008.10.011.
- 403 Disney MI, Lewis P, Gomez-Dans J, Roy D, Wooster MJ, Lajas D (2011) 3D radiative transfer
404 modelling of fire impacts on a two-layer savanna system, *Remote Sensing of Environment*
405 **115**, 8, 1866-1881, doi: 10.1016/j.rse.2001.03.010.
- 406 Drewa PB (2003) Effects of fire season and intensity on *Prosopis glandulosa* Torr. var.
407 *glandulosa*, *International Journal of Wildland Fire* **12**, 2, 147-157, doi: 10.1071/WF02021.
- 408 Eidenshink J, Schwind B, Brewer K, Zhu Z, Quayle B, Howard S (2007) A project for
409 monitoring trends in burn severity, *Journal of Fire Ecology* **3**, 1, 3-21.
- 410 Freeborn PH, Wooster MJ, Min Hao W, Ryan CA, Nordgren BL, Baker AP, Ichoku C (2008)
411 Relationships between energy release, fuel mass loss, and trace gas and aerosol emissions
412 during laboratory biomass fires, *Journal of Geophysical Research* **113**, D01301,doi:
413 10.1029/2007jd008679.
- 414 Freeborn PH, Wooster MJ, Roberts G (2011) Addressing the spatiotemporal sampling design of
415 MODIS to provide estimates of the fire radiative energy emitted from Africa, *Remote*
416 *Sensing of Environment* **115**, 2, 475-489.
- 417 French NHF, Kasischke ES, Hall RJ, Murphy KA, Verbyla DL, Hoy EE, Allen JL (2008) Using
418 Landsat data to assess fire and burn severity in the North American boreal forest region: an
419 overview and summary of results, *International Journal of Wildland Fire* **17**, 4, 443-462,
420 doi: 10.1071/WF08007.

- 421 Giglio L, Kendall JD, Justice CO (1999) Evaluation of global fire detection algorithms using
422 simulated AVHRR infrared data, *International Journal of Remote Sensing* **20**, 10, 1947 -
423 1985.
- 424 Giglio L, Descloitres J, Justice CO, Kaufman YJ (2003) An enhanced contextual fire detection
425 algorithm for MODIS, *Remote Sensing of Environment* **87**, 2-3, 273-282, doi:
426 10.1016/S0034-4257(03)00184-6.
- 427 Giglio L (2010) MODIS Collection 5 Active Fire product User's Guide, Version 2.4, SSAI,
428 61pp.
- 429 Giglio L, Randerson JT, van der Werf GR, Kasibhatla PS, Collatz GJ, Morton DC, DeFriesRS
430 (2010) Assessing variability and long-term trends in burned area by merging multiple
431 satellite fire products, *Biogeosciences* **7**, 1171-1186, doi: 10.5194/bg-7-1171-2010.
- 432 Goetz SJ, Mack MC, Gurney KR, Randerson JT, Houghton RA (2007) Ecosystem responses to
433 recent climate change and fire disturbance at northern high latitudes: Observations and
434 model results contrasting northern Eurasia and North America, *Environmental Research*
435 *Letters* **2**, 4, 045031, doi: 10.1088/1748-9326/2/4/045031.
- 436 Hartford RA, Frandsen WH (1992) When it's hot, it's hot- or maybe it's not! (surface flaming
437 may not portend extensive soil heating), *International Journal of Wildland Fire* **2**,3, 139-
438 144, doi: 10.1071/WF9920139.
- 439 Ichoku C, Kaufman YK (2005) A method to derive smoke emission rates from MODIS fire
440 radiative energy measurements, *IEEE Transactions on Geosciences and Remote Sensing*
441 **11**,43, 2636-2649.

- 442 Ju J, Roy DP, Vermote E, Masek J, Kovalskyy V (2012) Continental-scale validation of MODIS-
443 based and LEDAPS Landsat ETM+ atmospheric correction methods, *Remote Sensing of*
444 *Environment*, Landsat Legacy Special Issue, *Remote Sensing of Environment* **122**, 175–184.
- 445 Kaufman YJ, Remer LA, Ottmar RD, Ward DE, Li RR, Kleidman R, Fraser RA, Flynn L,
446 McDougal D, Shelton G (1996) Relationship between remotely sensed fire intensity and rate
447 of emission of smoke: SCAR-C experiment, in *Global Biomass Burning*, Edi. JS Levine, pp.
448 685–696, MIT Press, Cambridge, Mass.
- 449 Kaufman YJ, Justice CO, Flynn LP, Kendall JD, Prins EM, Giglio L, Ward DE, Menzel WP,
450 Setzer AW (1998) Potential global fire monitoring from EOS-MODIS, *Journal of*
451 *Geophysical Research* **103**, D24, 32215-32238, doi: 10.1029/98JD01644.
- 452 Keeley JE, Brennan T, Pfaff AH (2008) Fire severity and ecosystem responses following crown
453 fires in California shrublands, *Ecological Applications* **18**,1530–1546, doi: 10.1890/07-
454 0836.1.
- 455 Keeley JE (2009) Fire intensity, fire severity and burn severity: A brief review and suggested
456 usage, *International Journal of Wildland Fire* **18**, 1,116-126, doi: 10.1071/WF07049.
- 457 Key CH, Benson NC (2006) Landscape assessment: Ground measure of severity, the Composite
458 Burn Index; and remote sensing of severity, the Normalized Burn Ratio. In ‘FIREMON:
459 Fire Effects Monitoring and Inventory System.’ (Eds. DC, Lutes, RE, Keane, JF, Caratti,
460 CH, Key, NC, Benson, S, Sutherland, LJ, Gangi), USDA Forest Service, Rocky Mountain
461 Research Station General Technical Report, RMRS-GTR-164-CD: LA 1-51. (Ogden, UT).
- 462 Kremens RL, Smith AMS, Dickinson MB (2010) Fire metrology: current and future directions in
463 physics-based measurements, *Fire Ecology* **6**, 1, 13-35.

- 464 Kremens RL, Dickinson MB, Bova AS (2012) Radiant flux density, energy density and fuel
465 consumption in mixed-oak forest surface fires, *International Journal of Wildland Fire* **21**,
466 6, 722-730.
- 467 Kumar SS, Roy DP, Boschetti L, Kremens R (2011) Exploiting the power law distribution properties
468 of satellite fire radiative power retrievals - a method to estimate fire radiative energy and
469 biomass burned from sparse satellite observations, *Journal of Geophysical Research* **116**,
470 D19303, doi:10.1029/2011JD015676.
- 471 Lee DS, Storey JC, Choate MJ, Hayes R (2004). Four years of Landsat-7 on-orbit geometric
472 calibration and performance. *IEEE Transactions on Geoscience and Remote Sensing* **42**,
473 2786–2795.
- 474 Lentile LB, Holden ZA, Smith AMS, Falkowski MJ, Hudak AT, Morgan P, Lewis SA, Gessler
475 PE, Benson NC (2006) Remote sensing techniques to assess active fire and post-fire effects,
476 *International Journal of Wildland Fire* **15**, 3, 319-345, doi: 10.1071/WF05097.
- 477 Lentile LB, Smith AMS, Hudak AT, Morgan P, Bobbitt MJ, Lewis SA, Robichaud PR (2009)
478 Remote sensing for prediction of 1-year post-fire ecosystem condition, *International*
479 *Journal of Wildland Fire* **18**, 5, 594-608, doi: 10.1071/WF07091.
- 480 Littell JS, McKenzie D, Peterson DL, Westerling AL (2009) Climatic influences on twentieth-
481 century area burned in ecoprovinces of the western U.S., *Ecological Applications* **19**, 4,
482 1003-1021, doi: 10.1890/07-1183.1.
- 483 López Garcia MJ, Caselles V (1991) Mapping burns and natural reforestation using Thematic
484 Mapper data, *Geocarto International* **6**, 1,31–37, doi: 10.1080/10106049109354290.

- 485 McCool SF, Burchfield JA, Carroll MS (2006) An event-based approach for examining the
486 effects of wildland fire decisions on communities, *Environmental Management* **37**, 4, 437-
487 450.
- 488 Miller JD, Yool SR (2002) Mapping forest post-fire canopy consumption in several overstory
489 types using multi-temporal Landsat TM and ETM data. *Remote Sensing of Environment* **82**,
490 481-496.
- 491 Miller JD, Thode AE (2007) Quantifying burn severity in a heterogeneous landscape with a
492 relative version of the delta Normalized Burn Ratio (dNBR), *Remote Sensing of*
493 *Environment* **109**, 1,66-80, doi: 10.1016/j.rse.2006.12.006.
- 494 Miller JD, Safford HD, Crimmins M, Thode AE (2008) Quantitative evidence for increasing
495 forest fire severity in the Sierra Nevada and Southern Cascade Mountains, California and
496 Nevada, USA, *Ecosystems* doi: 10.1007/s10021-008-9201-9.
- 497 Morgan P, Hardy CC, Swetnam TW, Rollins MG, Long DG (2001) Mapping fire regimes across
498 time and space: Understanding coarse and fine-scale fire patterns, *International Journal of*
499 *Wildland Fire* **10**, 4, 329-342, doi: 10.1071/WF01032.
- 500 Pavaglio TB, Jakes PJ, Carroll MS, Williams DR (2009) Understanding social complexity within
501 the Wildland-Urban Interface: A new species of human habitation? *Environmental*
502 *Management* **43**, 6, 1085-1095, doi: 10.1007/s0026-009-9282-z.
- 503 Roberts G, Wooster MJ, Lagoudakis E (2009) Annual and diurnal African biomass burning
504 temporal dynamics, *Biogeosciences* **6**, 5,849–866, doi:10.5194/bg-6-849-2009.
- 505 Robichaud PR (2004) Postfire rehabilitation treatments: are we learning what works?, *Southwest*
506 *Hyrdology* **5**, 20-21.

- 507 Robichaud PR (2009) Post-fire Stabilization and Rehabilitation, In: Fire Effects on Soils and
508 Restoration Strategies, Science Publishers, Enfield, NH, USA.
- 509 Rothermel RC (1972) A mathematical model for predicting fire spread in wildland fuels, USDA
510 Forest Service, Research Paper INT-115.40p.
- 511 Roy DP, Boschetti L, Trigg S (2006) Remote sensing of fire severity: assessing the performance
512 of the normalized burn ratio, *IEEE Geoscience and Remote Sensing Letters* **3**, 1, 112-116.
- 513 Roy DP, Landmann T (2005) Characterizing the surface heterogeneity of fire effects using multi-
514 temporal reflective wavelength data, *International Journal of Remote Sensing* **26**, 19, 4197-
515 4218, doi: 10.1080/01431160500112783.
- 516 Roy DP, Boschetti L, Maier SW, Smith AMS (2010) Field estimation of ash and char color-
517 lightness using a standard gray scale, *International Journal of Wildland Fire* **19**, 6, 698-
518 704, doi: 10.1071/WF09133.
- 519 Roy DP, Boschetti L, Justice CO, Ju J (2008) The collection 5 MODIS burned area product –
520 global evaluation by comparison with the MODIS active fire product, *Remote Sensing of*
521 *Environment* **112**, 9, 3690–3707, doi: 10.1016/j.rse.2008.05.013.
- 522 Ryan KC (2002) Dynamic interactions between forest structure and fire behavior in boreal
523 ecosystems, *Silva Fennica* **36**, 1, 13–39.
- 524 Ryan KC, Noste NV (1985) Evaluating prescribed fires. In ‘Proceedings of the symposium and
525 workshop on wilderness fire. 1983 November 15-18, Missoula Montana’ (Eds. JE Lotan,
526 BM Kilgore, WC Fischer, RW Mutch) USDA Forest Service, Intermountain Forest and
527 Range Experiment Station General Technical Report INT-GTR-182 (Ogden, UT) pp. 230-
528 238.

- 529 Schroeder W, Csiszar I, Giglio L, Schmidt CC (2010) On the use of fire radiative power, area,
530 and temperature estimates to characterize biomass burning via moderate to coarse spatial
531 resolution remote sensing data in the Brazilian Amazon, *Journal of Geophysical Research*
532 **115**, D21, D21121.
- 533 Smith AMS, Wooster MJ (2005) Remote classification of head and backfire types from MODIS
534 fire radiative power and smoke plume observations, *International Journal of Wildland Fire*
535 **14**, 3, 249-254.
- 536 Smith AMS, Wooster MJ, Drake NA, Dipotso FM, Falkowski MJ, Hudak AT (2005) Testing the
537 potential of multi-spectral remote sensing for retrospectively estimating fire severity in
538 African Savannas, *Remote Sensing of Environment* **97**, 1, 92-115, doi:
539 10.1016/j.rse.2005.04.014.
- 540 Smith AMS, Lentile LB, Hudak AT, Morgan P (2007) Evaluation of linear spectral unmixing
541 and dNBR for predicting post-fire recovery in a North American ponderosa pine forest,
542 *International Journal of Remote Sensing* **22**, 20, 5159-5166, doi:
543 10.1080/01431160701395161.
- 544 Smith AMS, Eitel JUH, Hudak AT (2010) Spectral analysis of charcoal on soils: implications for
545 wildland fire severity mapping methods, *International Journal of Wildland Fire* **19**, 976–
546 983, doi: 10.1071/WF09057.
- 547 Sullivan AL (2009a) Wildland surface fire spread modeling, 1990–2007. 1: Physical and quasi-
548 physical models, *International Journal of Wildland Fire* **18**, 4, 349-368, doi:
549 10.1071/WF06143.

- 550 Sullivan AL (2009b) Wildland surface fire spread modelling, 1990–2007. 2: Empirical and
551 quasi-empirical models, *International Journal of Wildland Fire* **18**, 4, 369-386, doi:
552 10.1071/WF06142.
- 553 Sullivan AL (2009c) Wildland surface fire spread modelling, 1990–2007. 3: Simulation and
554 mathematical analogue models, *International Journal of Wildland Fire* **18**, 4, 387-403, doi:
555 10.1071/WF06144.
- 556 Trollope WSW, Tainton NM (1986) Effect of fire intensity on the grass and bush components of
557 the Eastern Cape thornveld, *African Journal of Range and Forage Science* **3**, 37–42.
- 558 van der Werf GR, Randerson JT, Giglio L, Collatz GJ, Mu M, Kasibhatla PS, Morton DS,
559 DeFries RS, Jin Y, van Leeuwen TT (2010) Global fire emissions and the contribution of
560 deforestation, savanna, forest, agricultural, and peat fires (1997–2009), *Atmospheric*
561 *Chemistry & Physics Discussions* **10**, 16153–16230, doi: 10.5194/acpd-10-16153-2010.
- 562 Westerling AL, Hidalgo HG, Cayan DR, Swetnam TW (2006) Warming and earlier spring
563 increase western U.S. forest wildfire activity, *Science* **313**, 5789, 940-943, doi:
564 10.1126/science.1128834.
- 565 Wolfe RE, Roy DP, Vermote E (1998), MODIS land data storage, gridding, and compositing
566 methodology: Level 2 grid, *Geoscience and Remote Sensing, IEEE Transactions on*
567 *Geosciences and Remote Sensing* **36**, 4, 1324-1338.
- 568 Wolfe RE, Nishihama M, Fleig A, Kuyper J, Roy DP, Storey J, Patt F (2002). Achieving sub-
569 pixel geolocation accuracy in support of MODIS land science, *Remote Sensing of*
570 *Environment* **83**, 31-49.

571 Wooster MJ (2002) Small-scale experimental testing of fire radiative energy for quantifying
572 mass combusted in natural vegetation fires, *Geophysical Research Letters* **29**, 21, 2027,
573 doi:10.1029/2002GL015487.

574 Wooster MJ, Zhang YH (2004) Boreal forest fires burn less intensely in Russia than in North
575 America, *Geophysical Research Letters* **31**, L20505, doi: 10.1029/2004GL020805.

576 Wooster MJ, Roberts G, Perry GLW, Kaufman YJ (2005) Retrieval of biomass combustion rates
577 and totals from fire radiative power observations: FRP derivation and calibration
578 relationships between biomass consumption and fire radiative energy release, *Journal of*
579 *Geophysical Research* **110**, D24, D24311.

580

581

582

583

584

585

586

587

588

589

590

Table 1. Common metrics for inferring burn severity from satellite imagery.

Spectral Index	Equation	Reference
Normalized Burn Ratio	$NBR = (\rho_4 - \rho_7) / (\rho_4 + \rho_7)$	Key and Benson, 2006
Differenced Normalized Burn Ratio	$dNBR = NBR_i - NBR_f$	Key and Benson, 2006
Relative Differenced Normalized Burn Ratio	$RdNBR = dNBR / \sqrt{ABS(NBR_i / 1000)}$	Miller and Thode, 2007

Key: ρ_4 and ρ_7 are the top-of-atmosphere spectral reflectance as measured in bands 4 (0.76 - 0.90 μm) and 7 (2.08 - 2.35 μm) of the Landsat Enhanced Thematic Mapper (ETM+) sensor, i denotes pre-fire imagery, and f denotes post-fire imagery.

591

592

593 **Table 2.** Significant relationships between metrics of burn severity (dNBR and RdNBR) and
 594 distributional metrics of fire radiative power (median and 90th percentile) overall and within two
 595 tree canopy closure percentage classes ($\alpha=0.05$). No significant relationships were found
 596 between burn severity metrics and maximum MODIS FRP.

597

	Median FRP				90 th Percentile FRP			
	r ²	n	F	SE	r ²	n	F	SE
dNBR								
Overall	-	-	-	-	-	-	-	-
25-60%	*0.43	10	6.1	81	*0.49	10	7.8	77
60-100%	-	-	-	-	-	-	-	-
RdNBR								
Overall	-	-	-	-	^β 0.42	13	8.0	127
25-60%	*0.63	10	13.6	135	*0.69	10	18	122
60-100%	-	-	-	-	-	-	-	-

* linear relationship

^β logarithmic relationship

599

600

601

602

603

604

605

606

607

608 **Figure Captions:**

609

610 **Fig. 1.** Locations of the sixteen fires in the western United States.

611

612 **Fig.2.** Scatterplots of mean dNBR and RdNBR with co-located 1-km MODIS FRP observations
613 for data (n=1716) from all 16 fires.

614

615 **Fig. 3.** Scatterplots of mean RdNBR with 1-km MODISFRP observations for data from four of
616 the fires (Middle fork fire, n= 71; Columbia complex fire, n=642, Hunter fire, n=178, Red
617 Mountain fire, n=125) and across four vegetation types (Herbaceous grassland, n=95,
618 Herbaceous shrub steppe, n=21, Open Tree Canopy, n=606, Closed Tree Canopy, n=904).All
619 twelve other fires showed similar patterns.

620

621 **Fig. 4** Mean Landsat derived RdNBR for each fire (error bars show standard error of the mean)
622 plotted against metrics of MODIS 1-km FRP for all active fire detections. MODIS FRP metrics
623 plotted are (a) 90th percentile MODIS FRP for all fires with greater than 10 samples (n=13), (b)
624 90th percentile MODIS FRP for each fire stratified by high (60-100%, n=13) and moderate (25-
625 60%, n=10) tree cover class types, (c) Median MODIS FRP for each fire stratified by high (60-
626 100%, n=13) and moderate (25-60%, n=10) tree cover class types. Insufficient MODIS FRP
627 points and/or individual fires were available in low tree cover classes (<25%, n=3) to enable a
628 rigorous investigation.

629

630

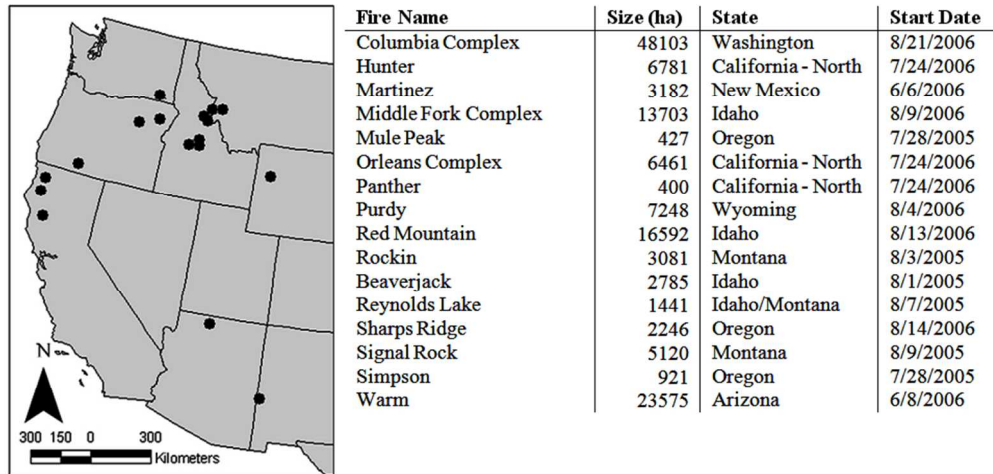


Fig. 1. Locations of the sixteen fires in the western United States.
339x165mm (72 x 72 DPI)

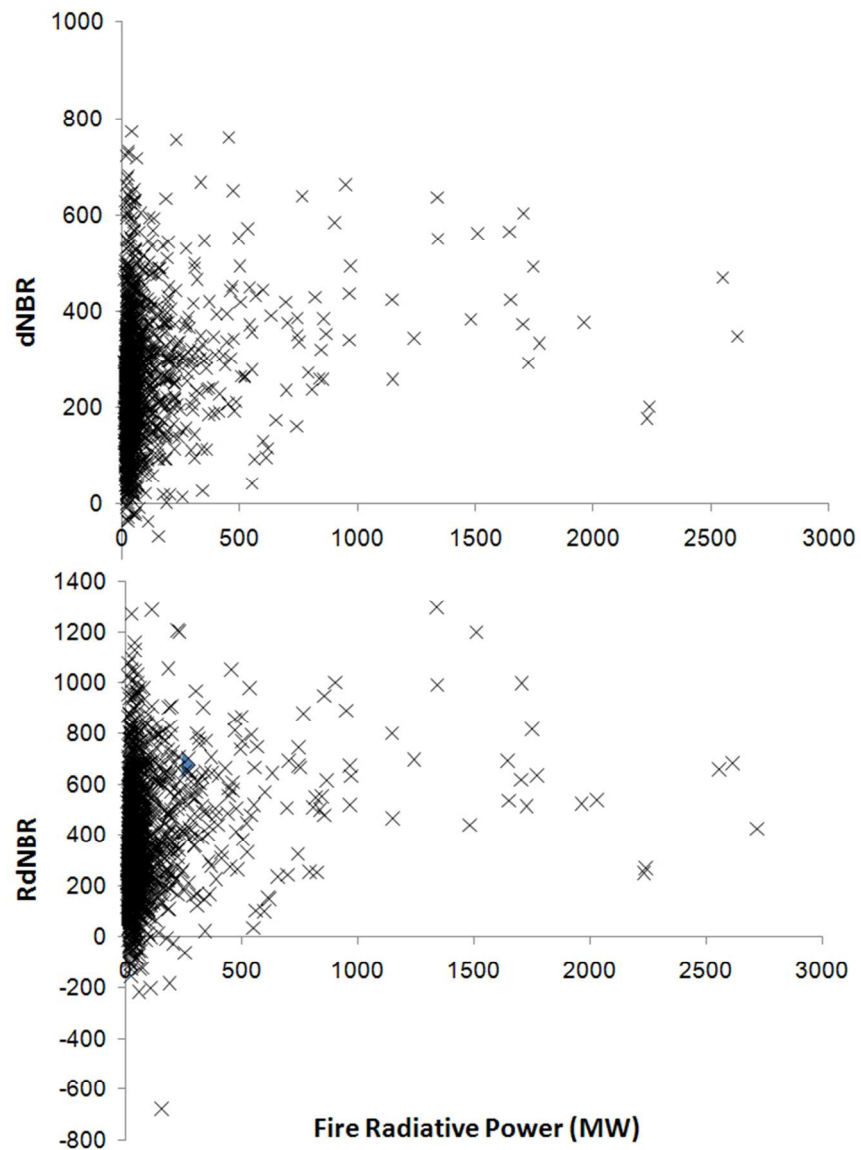


Fig.2. Scatterplots of mean dNBR and RdNBR with co-located 1-km MODIS FRP observations for data (n=1716) from all 16 fires. 256x346mm (72 x 72 DPI)

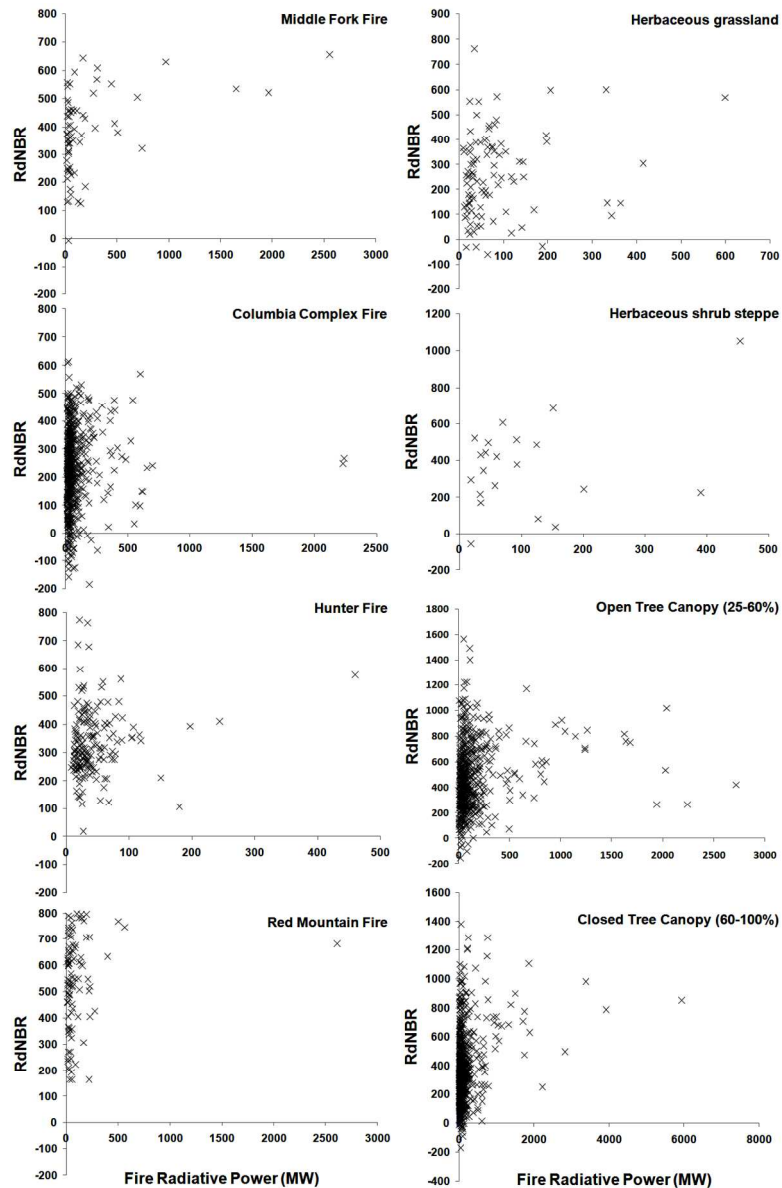


Fig. 3. Scatterplots of mean RdNBR with 1-km MODISFRP observations for data from four of the fires (Middle fork fire, $n=71$; Columbia complex fire, $n=642$, Hunter fire, $n=178$, Red Mountain fire, $n=125$) and across four vegetation types (Herbaceous grassland, $n=95$, Herbaceous shrub steppe, $n=21$, Open Tree Canopy, $n=606$, Closed Tree Canopy, $n=904$). All twelve other fires showed similar patterns.
479x732mm (72 x 72 DPI)

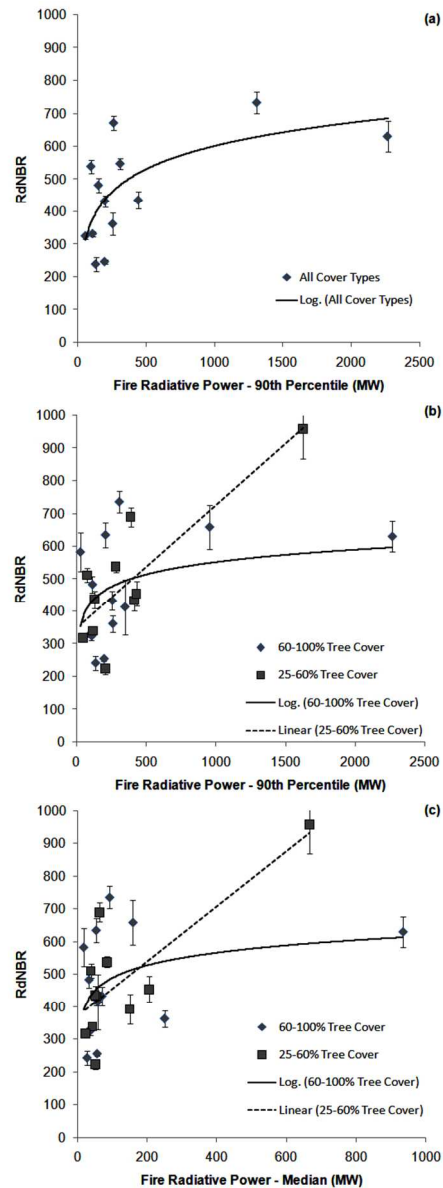


Fig. 4 Mean Landsat derived RdNBR for each fire (error bars show standard error of the mean) plotted against metrics of MODIS 1-km FRP for all active fire detections. MODIS FRP metrics plotted are (a) 90th percentile MODIS FRP for all fires with greater than 10 samples ($n=13$), (b) 90th percentile MODIS FRP for each fire stratified by high (60-100%, $n=13$) and moderate (25-60%, $n=10$) tree cover class types, (c) Median MODIS FRP for each fire stratified by high (60-100%, $n=13$) and moderate (25-60%, $n=10$) tree cover class types. Insufficient MODIS FRP points and/or individual fires were available in low tree cover classes ($<25\%$, $n=3$) to enable a rigorous investigation.

194x511mm (72 x 72 DPI)